Journal of Nano- and Electronic Physics
Vol. 8 No 1, 01042(4pp) (2016)

Журнал нано- та електронної фізики
Том 8 № 1, 01042(4cc) (2016)

Structural Engineering of the Vacuum Arc ZrN/CrN Multilayer Coatings

O.V. Sobol'[1,*], A.A. Andreev[2], V.F. Gorban'[3], A.A. Meylekhov[1], H.O. Postelnyk[1], V.A. Stolbovoy[2]

[1] *National Technical University "Kharkiv Polytechnic Institute", 21, Frunze St., 61002 Kharkiv, Ukraine*
[2] *National Science Center "Kharkov Institute of Physics and Technology", 1, Akademicheskaya St., 61108 Kharkiv, Ukraine*
[3] *Frantsevich Institute for Problems of Materials Science, 3, Krzhizhanovsky St., 03680 Kyiv, Ukraine*

(Received 04 February 2016; revised manuscript received 02 March 2016; published online 15 March 2016)

The influence of the layer thickness (in the nanometer range) and negative bias potential ($-U_s$) supplied during the deposition on the structure and hardness of the composite vacuum-arc coatings are analyzed for multilayer ZrN/CrN system with a large difference in the atomic weights and radiation-induced defect formation of metal components. It is established that at the layer thickness less than 50 nm, supply of $-U_s$ leads to an increase of microstrain in the CrN layers under bombardment by Zr ions with large atomic radius and mass, and the strain relaxation is observed in ZrN layers. The observed effects are explained by an increase in energy of deposited ionized particles when applying $-U_s$ that determines the radiation-induced mixing at the interphase boundaries of the layers and leads to the hardness decrease. The highest hardness of 42 GPa in the ZrN/CrN system is achieved upon deposition of thin (20 nm) layers in the absence of $-U_s$.

Keywords: Multilayer coating, ZrN/CrN, Layer thickness, Implantation, Mixing, Structure, Microstrain, Hardness.

DOI: 10.21272/jnep.8(1).01042 PACS numbers: 81.07.Bc, 61.05.cp, 68.55.jm, 61.82.Rx

Multilayer systems allow to artificially create and strictly control the nanoscale structural state due to the fixed thickness of alternating layers with different phase composition and structural state [1-8]. From this it follows that the state of the interface boundary is a very important factor determining the functional properties of a multilayer coating. This becomes especially relevant when the layer thickness reaches nanometer size that allows to significantly increase the mechanical properties of coatings [9-11]. Nitrides of transition metals of the IV-th (Ti, Zr) and VI-th (Cr, Mo) groups [3, 12], among which ZrN/CrN system possesses the greatest hardness of the components, have good prospects for use as the constituents of a multilayer system (the nanoscale layer thickness of which allows to obtain high hardness and wear resistance).

For forecasting production of the necessary properties of such systems, it is important to establish the basic (for structural engineering) relationship between the phase composition, size, and orientation of crystallites, their micro- and macrostrain state depending on the formation conditions, among which the most critical for multilayer systems are the following [1, 3]: working atmosphere pressure, layer thickness, and bias potential supplied in the deposition. The criticism of the latter is caused by the possibility of mixing in the layers, which are small in thickness, during deposition that significantly influences the properties of the multilayer composition.

Therefore, the aim of the present work was to perform the comparative analysis for the ZrN/CrN system of the regularities of structural engineering in both the constituent layers and multilayer composition taking into account the simulation results of radiation-induced defect formation and its impact on the stress-strain state and mechanical properties.

METHODS OF PRODUCTION AND STUDY OF THE SAMPLES

Multilayer two-phase nanostructured CrN-ZrN coatings were deposited in the vacuum-arc device "Bulat-6" [12]. The following materials were used as the cathode ones: chromium and weakly doped zirconium, nitrogen (active gas) (99.95 %). The coatings were deposited from two metal sources (Cr and Zr) on the samples surface of $20 \times 20 \times 2$ mm of 12Х18Н10Т steel.

The coatings were prepared by both the continuous rotation of the holder with the speed of 8 rev/min and number of layers of 540-570 and a fixed stop on time of 10, 20, 40, or 150 s near each of two cathodes to obtain thicker layers.

The deposition process was implemented at the following technological conditions: arc current during deposition was 100 A, nitrogen pressure (P_N) in the chamber varied in the range of 10^{-5}...$5 \cdot 10^{-3}$ torr, distance from the evaporator to the substrate was equal to 250 mm, and substrate temperature (T_{sub}) belonged to the range of 250...350 °C. The coatings of about 10 μm thickness were obtained when applying a constant negative potential ($-U_s$) of the value of – 120 V and – 150 V and also without feeding $-U_s$.

Multilayer nanostructured CrN-ZrN coatings with the stimulation of the mobility of deposited atoms were fabricated by applying to the substrate-holder a high-voltage potential ($-U_i$) in the pulse form with the pulse duration of 10 μs, pulse repetition frequency of 7 kHz, and amplitude of – 1200 V [13].

To calculate the ion free path and vacancy distribution in CrN and ZrN layers of the coating, the program package SRIM was used [14].

Phase composition, structure, and substructural characteristics were studied by X-ray diffractometry method (DRON-4) with Cu-K_α-radiation. Graphite monochroma-

* sool@kpi.kharkov.ua

tor placed in the secondary beam (in front of the detector) was used for monochromatization of the recorded radiation. The study of the phase composition, structure (texture, substructure) was carried out using the traditional techniques of X-ray diffractometry by the analysis of the positon, intensity, and shape of diffraction reflection profiles. Interpretation of the diffraction patterns was conducted using the tables of the International Powder Diffraction File Center. The substructural characteristics were defined by the approximation method [15, 16].

The surface morphology and elemental composition were studied on the scanning electron microscope JEOL JSM-840 with EDX.

Microindentation was performed on the "Micron-gamma" device with the load to $F = 0.5$ N by the Bercovich diamond pyramid with the sharpening angle of 65°, with automatic loading and uploading during 30 s [17, 18].

RESULTS AND DISCUSSION

The study of the fracture morphology of the ZrN/CrN coatings has shown a high planarity of the layers and practically the absence of the droplet phase in the bulk of the multilayer coating for composite multilayer coatings with different layer thickness. In Fig. 1 we present the lateral cross-sections, from which one can clearly see the presence of the droplet phase on the surface and its practical absence on the coating cross-section. It is also seen that CrN (light) and ZrN (dark) layers are close to each other in thickness and agree well in absolute magnitude with the calculated values of 600 nm for the 12-layer condensate (see Fig. 1a) and about 300 nm for the 24-layer one (Fig. 1b).

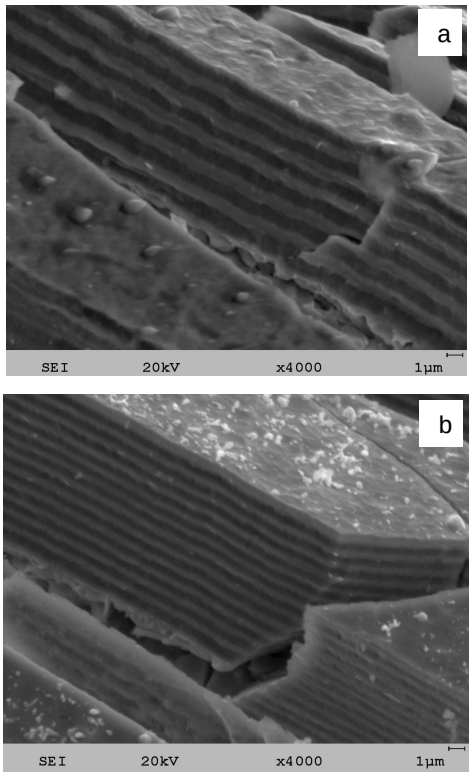

Fig. 1 – Side view of the layers of composite ZrN/CrN coatings with the number of layers of 12 and layer thickness of 600 nm (a) and number of layers of 24 and layer thickness of 300 nm (b)

The next stage of establishing regularities necessary for structural engineering was based on the investigation of the influence of the deposition conditions on the structure and properties of the CrN component as the least structurally stable to the deposition conditions and post-condensation exposure [19]. Formation of the Cr_2N and CrN phases in different proportions (specific content of CrN increases with increasing P_N) occurs in chromium nitride layers in the studied operating pressure range of $(7…48)\cdot10^{-4}$ torr. The average crystallite size is equal to 6-8 nm at the substructural level in the coatings obtained at low pressures. At high P_N, when the texture [111] formation occurs and the compression stresses of the value of – 2.8 GPa are developed in the growth plane, the average crystallite size in the direction of the texture axis increases to 15 nm.

Supply of an additional high-voltage negative pulse potential leads to the increase in the average crystallite size by 15-20 %. At that, microstrain is equal to 0.25-0.3 %. We should note that a high-voltage pulse impact stimulates the nitride formation and formation of stoichiometric mononitride at lower pressures [20, 21]. The latter is manifested in the dependence of the hardness in the form of practically constant values for the whole range of P_N (Fig. 2, dependence 2).

For the coatings obtained without high-voltage pulse action, the dependence of hardness is nonmonotonic (see Fig. 2, dependence 1) with the minimal value of 21 GPa at small P_N, when the coating is almost single-phase (low nitride Cr_2N), with the largest value of 32 GPa for the two-phase (Cr_2N + CrN) composition, and decrease in hardness at higher pressure, for which the increase in the average crystallite size occurs.

The component of zirconium nitride in the considered range of P_N has only single-phase ZrN state, at which P_N growth is accompanied by the appearance of the texture [111]. Increase in the size of crystallites (up to 110 nm) and stabilization of microstrain at the level of 0.5 % are observed for the highest pressure of $4.8\cdot10^{-3}$ torr at the substructural level as well as for CrN. Hardness of such coatings is approximately equal to 35 GPa.

The use of scanning electron microscopic studies in combination with energy-dispersive analysis has shown that the nitrogen content in the formed phases is lower than the stoichiometric one even at the highest P_N used in the work. To the greatest extent, this applies to the Cr-N system, where the nitrogen content is 32.13 wt. % without the high-frequency pulse effect and 34.88 wt. % in the formation with the pulse impact. In ZrN, nonstoichiometry is less considerable: Zr – 54.83 wt. % and N – 45.17 wt. % that corresponds to the $ZrN_{0.78}$ formula.

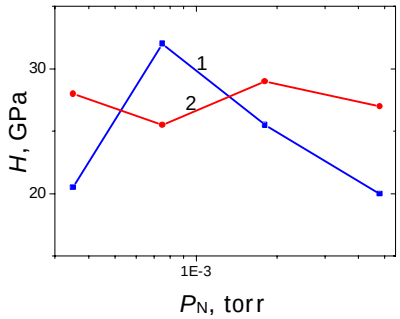

Fig. 2 – Dependence of the hardness of the coatings obtained at different P_N: 1) – U_s = – 120 V, 2) – U_s = – 120 V, U_i = – 1200 V

The state of the interface boundaries of a multilayer composition formed on the basis of these two systems of nitrides is very important. Modeling of processes which can occur on the boundary at the nanometer size of the layers is based on the radiation-induced processes during deposition. Using the program package SRIM, the implantation modeling showed that in the case of irradiation with ions of the average energy of 150 eV that corresponds to deposition of singly charged ions under the action of $-U_s = -150$ V, in the case of bombardment Cr → ZrN, the maximum of the ion distribution is located on the depth of ≈ 0.8 nm, and of the vacancy distribution – 0.3 nm with the density in the maximum of 0.7 vac/ion (for 10 iterations). In the opposite case of the initial growth stages of the zirconium nitride layer on the chromium nitride layer, i.e. when Zr → CrN, the maximum of the ion distribution is located on the depth of ≈ 1 nm and of vacancies – 0.5 nm with the density in the maximum of 0.8 vac/ion. Thus, the boundary between the growing layer of zirconium nitride on CrN is more exposed to radiation, at that, the efficiency of this exposure is higher due to the much larger not only the atomic mass, but also the atomic radius of zirconium (0.16 nm for Zr and 0.13 nm for CrN).

The radiation exposure has the greatest effect on the macro- and microstrain state of the coatings [11, 20, 22].

Using the multiple inclined survey method ($\sin^2\psi$-method) [15], the conducted analysis of the macrostress-strain state for individual ZrN and CrN layers of multilayer ZrN/CrN composition has shown that the compressive stresses are developed in both layers and the crystal lattice is compressed in the layer growth plane. To the greatest extent, the compressive macrostrain (reaching the value of 3 %, see Fig. 3) is exhibited for the smallest layer thickness, when the effect of implantation is most pronounced.

At the substructural level, the size of crystallites was proportional to the layer thickness, and the microstrain varied differently in CrN and ZrN layers (Fig. 4). With increasing thickness, the microstrain increases in CrN and decreases in ZrN layers.

Such behavior of the dependences can be associated with radiation damage that is most pronounced in thin layers comparable with the impact depth. Then, a less effect of Cr to ZrN (as follows from the above results of model calculations) should be exhibited in a less strain of the crystal lattice, and a greater influence in the case of Zr introduction into CrN layers – to a larger strain that is observed in Fig. 4.

We note that when applying pulse potential (without supply of $-U_s$), the microstrain decreases in both cases with decreasing thickness that implies the determining influence of the constantly acting potential compared with the pulse effect even at a significantly greater (in the absolute value) amplitude of the applied pulse potential. At that, the pulse duration of high-voltage impact was approximately equal to 9 % of the relaxation time.

Radiation exposure has a decisive influence on such a universal mechanical characteristic of the coating as hardness. As seen from Fig. 5, in the case of thin layers of the nanoscale value, the absence of constantly acting high-energy ion mixing (dependence 1 in Fig. 5) leads to the increase in hardness with decreasing layer thickness (the size effect [1, 3]). At the same time, deposition upon

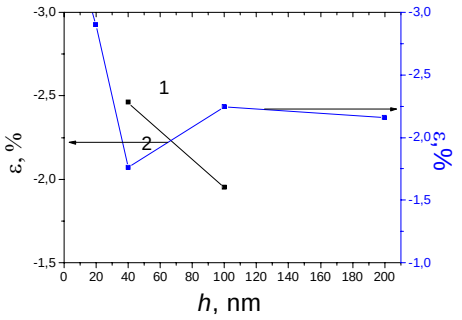

Fig. 3 – Macrostrain in the layers of the thickness of h for the CrN (1) and ZrN (2) layers of the composite coating

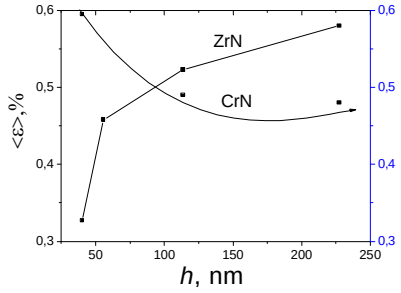

Fig. 4 – Dependence of the microstrain $\langle\varepsilon\rangle$ on the thickness of ZrN and CrN layers for the coatings obtained at $-U_s = -150$ V and $-U_i = -0$ V

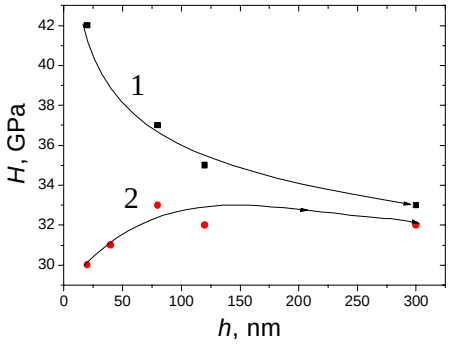

Fig. 5 – Dependence of the ZrN/CrN composite hardness on the layers thickness during the deposition without $-U_s$ (1) and with $-U_s = -150$ V (2) ($P_N = 4.8 \cdot 10^{-3}$ torr)

fast ion bombardment when applying $-U_s$ results in the reduction of the coating hardness with decreasing layer thickness (dependence 2, Fig. 5) that can be determined by mixing at the interphase boundary due to the implantation processes.

Thus, the effect of increasing mechanical properties with the decrease in the layers thickness to nanometer size in a multilayer composition can be implemented in the case of low mixing at the interphase boundary of the layers that for strongly different masses of the metals, which are the constituents of layers, as, for example, Zr and Cr in the work, can be achieved with a low bias potential, when the mixing process at the interphase boundary is insignificant. This is the fundamental difference from the previously most used TiN/CrN system with relatively close weights and low radiation damage of the metal components, for which the highest properties are achieved at a large bias potential [23] leading to the formation of preferentially oriented crystallites with the axis [111] under the action of the compressive stresses in the growth plane.

REFERENCES

1. *Nanostructured coatings* (Ed. by Cavaleiro Albano De Hosson, Jeff Th.M.) (Springer-Verlag: 2006).
2. P.H. Mayrhofer, C. Mitterer, L. Hultman, H. Clemens, *Prog. Mater. Sci.* 51, 1032 (2006).
3. E. Sheinman, *Metal Sci. Heat Treatment* 50 No 11-12, 600 (2008).
4. A. Gilewicz, B. Warcholinski, *Tribology Int.* 80, 34 (2014).
5. F.R. Lamastra, F. Leonardi, R. Montanari, F. Casadei, T. Valente, *Surf. Coat. Technol.* 200 No 22-23, 6172 (2006).
6. K. Lukaszkowicz, L.A. Dobrzański, A. Zarychta, L. Cunha, *J. Achievement. Mater. Manufactur. Eng.* 15 No 1-2, 47 (2006).
7. M.K. Samani, X.Z. Ding, N. Khosravian, B. Amin-Ahmadi, Yang Yi, G. Chen, E.C. Neyts, A. Bogaerts, B.K. Tay, *Thin Solid Films* 578, 133 (2015).
8. M. Ertas, A.C. Onel, G. Ekinci, B. Toydemir, S. Durdu, M. Usta, L. Colakerol, *J. Chem., Nuclear, Mater. Metallurgical Eng.* 9 No 1, 53 (2015).
9. R.A. Koshy, M.E. Graham, L.D. Marks, *Surf. Coat. Technol.* 202, 1123 (2007).
10. Harish C. Barshilia, Anjana Jain, K.S. Rajam, *Vacuum* 72, 241 (2004).
11. O.V. Sobol, O.N. Grigorjev, Yu.A. Kunitsky, S.N. Dub, A.A. Podtelezhnikov, A.N. Stetsenko, *Sci. Sintering* 38, 63 (2006).
12. A.A. Andreyev, L.P. Sobolev, S.N. Grigor′yev, *Vakuumno-dugovyye pokrytiya* (Kharkov: NNTs KhFTI: 2010).
13. O.V. Sobol′, A.A. Andreev, S.N. Grigoriev, V.F. Gorban′, M.A. Volosova, S.V. Aleshin, V.A. Stolbovoi, *Metal Sci. Heat Treatment* 54, No 3-4, 195 (2012).
14. http://www.srim.org/SRIM/Tutorials/Tutorials.htm
15. L.S. Palatnik, M.Ya. Fuks, V.M. Kosevich, *Mekhanizm obrazovaniya i substruktura kondensirovannykh plenok* (M.: Nauka: 1972).
16. O.V. Sobol′, *Phys. Solid State* 53 No 7, 1464 (2011).
17. E. Aznakayev, *Proc. Int. Conf. "Small Talk – 2003"* TP.001, 8 (San Diego, California, USA: 2003).
18. S.A. Firstov, V.F. Gorban′, N.A. Krapivka, E.P. Pechkovskiy, *Kompozity i nanomaterialy* No 2, 5 (2011).
19. O.V. Sobol′, A.A. Andreev, V.A. Stolbovoy, N.V. Pinchuk, A.A. Meylekhov, *J. Nano- Electron. Phys.* 7 No 1, 01026 (2015).
20. O.V. Sobol′, A.A. Andreev, S.N. Grigoriev, V.F. Gorban′, S.N. Volosova, S.V. Aleshin, V.A. Stolbovoy, *Problem. Atomic Sci. Technol.* No 4, 174 (2011).
21. N.A. Azarenkov, O.V. Sobol, V.M. Beresnev, A.D. Pogrebnyak, D.A. Kolesnikov, P.V. Turbin, U.M. Toruanyk, *Metallofiz. Nov. Tekhnol.* 35 No 8, 1061 (2013).
22. F. Lomello, M. Arab Pour Yazdi, F. Sanchette, F. Schuster, M. Tabarant, A. Billard, *Surf. Coat. Technol.* 238, 216 (2014).
23. O.V. Sobol′, A.A. Andreev, V.A. Stolbovoy, V.F. Gorban′, N.V. Pinchuk, A.A. Meylekhov, *J. Nano- Electron, Phys.* 7 No 1, 01034 (2015).